

Solar Influences on the North Atlantic Oscillation by Wavelet-Based Multifractal Analysis

Fumio Maruyama^{1*}, Kenji Kai², Hiroshi Morimoto²

¹Department of Sport and Health Science, Matsumoto University, Matsumoto, Japan

²Graduate School of Environmental Studies, Nagoya University, Nagoya, Japan

Email: *fmaruya@na.goya-u.jp

How to cite this paper: Maruyama, F., Kai, K. and Morimoto, H. (2018) Solar Influences on the North Atlantic Oscillation by Wavelet-Based Multifractal Analysis. *Journal of Geoscience and Environment Protection*, 6, 133-150.

<https://doi.org/10.4236/gep.2018.68010>

Received: June 18, 2018

Accepted: August 26, 2018

Published: August 29, 2018

Copyright © 2018 by authors and Scientific Research Publishing Inc.

This work is licensed under the Creative

Commons Attribution International

License (CC BY 4.0).

<http://creativecommons.org/licenses/by/4.0/>



Open Access

Abstract

There is increasing interest in the relation between the solar activity and climate change. Regarding the solar activity, the fractal property of the sunspot number (SSN) has been studied by many previous works. In general, fractal properties have been observed in the time series of the dynamics of complex systems. The purpose of this research is to investigate the relationship between the solar activity, total ozone, and the North Atlantic Oscillation (NAO) from a viewpoint of multi-fractality. To detect the changes of multi-fractality, we performed the wavelets analysis, and plotted the τ -function derived from the wavelets of these time series. We showed that the solar activity relate to the NAO, by observing the matching in monofractality or multifractality of these indices. When the SSN increased and the solar activity was stable, the NAO also became stable. When the SSN became maximum, the fractality of the SSN, F10.7 flux, geomagnetic aa, and NAO indices changed from multifractality to monofractality and those states became stable for most of the solar cycles. When the SSN became maximum, the fluctuations became large and multifractality became strong, and a change from multifractal to monofractal behavior was observed in the SSN, F10.7 flux, geomagnetic aa, and NAO indices. The strong interactions of the solar flux, geomagnetic activity, total ozone, and NAO occur in the SSN maximum. The strong interactions were inferred from the similarity of fractality changes and the wavelet coherence. The influence of the solar activity on the NAO was shown from a viewpoint of multi-fractality. These findings will contribute to the research on the effects of the solar activity on climate change.

Keywords

The Sunspot Number, Solar Radio Flux, Geomagnetic Activity, Total Ozone, NAO, Wavelet, Multifractal

1. Introduction

The influence of solar activity on climate has been discussed for a long time.

Recent measurements from space indicate that the total solar irradiance changes associated with the 11-year solar cycle are negligibly small (0.1%), although larger (4% - 8%) variations are found in the ultraviolet (UV) range of 200 - 250 nm [1]. Even if we do not expect direct solar cycle impacts at Earth's surface, a significant influence should be detected in the stratopause region [2]. The NAO is a seesaw of surface pressure in the eastern part of the North Atlantic between high latitudes and subtropics.

Recent advances in reconstruction of the past climate with fine temporal resolution clarified the relation between the solar cycles and the monsoon rainfall in South Oman with multiple time scales from decadal to millennial [3]. A decadal variation of tropical lower stratospheric ozone and temperature has previously been identified that correlates positively with the 11-year solar activity cycle. The El Niño-Southern Oscillation (ENSO) also influences lower stratospheric ozone and temperature [4].

A significant part of temperature variation could be the result of a solar wind interaction with the Earth's atmosphere and a subsequent modulation of the NAO [5]. Statistical analysis on the relationship between the solar and geomagnetic activities and the Arctic Oscillation is performed [6]. The correlation between the geomagnetic Ap and the NAO indices is high and significant since about 1970 [7]. The geomagnetic activity is fundamentally generated by the solar wind.

Various objects in nature show the so-called self-similarity or fractal property. Monofractal shows an approximately similar pattern at different scales and is characterized by a fractal dimension. Multifractal is a non-uniform, more complex fractal and is decomposed into many sub-sets characterized by different fractal dimensions. Fractal property can be observed in the time series representing dynamics of complex systems as well. A change of fractality accompanies a phase transition and changes of state. The multifractal properties of daily rainfall were investigated in two contrasting climates: an East Asian monsoon climate with extreme rainfall variability and a temperate climate with moderate rainfall variability [8]. In both the climates, the frontal rainfall shows monofractality and the convective-type rainfall shows multifractality.

Hence, climate change can be interpreted from the perspective of fractals. A change of fractality may be observed when the climate changes. We attempted to explain changes in climate, referred to as regime shifts, by analyzing fractality. We used the wavelet transform to analyze the multifractal behavior of the climate index. Wavelet methods are useful for the analysis of complex non-stationary time series. The wavelet transform allows reliable multifractal analysis to be performed [9]. In terms of the multifractal analysis, we conclude that a climatic regime shift corresponds to a change from multifractality to monofractality of the Pacific Decadal Oscillation (PDO) index [10] and we show

the influence of solar activity on the climatic regime shift [11].

This research method is an appropriate one for complex time series analysis.

We examined the influence of the solar activity on the NAO considering the total ozone and geomagnetic field. Moreover, we investigated the relationship among NAO, global temperature, and NH sea ice area. To detect the changes of multifractality, we examined the multifractal analysis on the SSN, solar radio flux at 10.7 cm (F10.7 flux), geomagnetic aa, NAO, total ozone, global temperature, and NH sea ice area indices using the wavelet transform. Besides we examined the wavelet coherence.

2. Data and Method of Analysis

The SSN provided by Solar Influences Data Analysis Center (sidc.oma.be), the F10.7 flux provided by NOAA's space weather prediction center (<https://www.swpc.noaa.gov/>) were used (Figure 1(a)). The F10.7 flux is an excellent indicator of the solar activity. The NAO index provided by NOAA's Climate Prediction Center, USA (CPC) was used (Figure 1(b)). The geomagnetic aa index provided by NOAA was used (Figure 1(c)) as the index of the solar activity, which was a measure of the disturbance level of the Earth's magnetic field based on magnetometer observations at two, nearly antipodal, stations in Australia and England. The total ozone provided by NASA (nasasearch.nasa.gov) were used (Figure 1(d)). The global average temperature anomalies obtained from the Met Office Hadley Centre was used (Figure 1(e)). We used the NSIDC Sea Ice Index which shows the NH sea ice area (Figure 1(f)).

We used the Daubechies wavelet as the analyzing wavelet because it is widely used in solving a broad range of problems, e.g., self-similarity properties of a signal or fractal problems and signal discontinuities. The data used were a discrete signal that fitted the Daubechies Mother wavelet with the capability of precise inverse transformation. Hence, precisely optimal value of $\tau(q)$ could be calculated as explained below. We then estimated the scaling of the partition function $Z_q(a)$, which is defined as the sum of the q -th powers of the modulus of the wavelet transform coefficients at scale a . In our study, the wavelet-transform coefficients did not become zero, and therefore, for a precise calculation, the summation was considered for the entire set. Muzy *et al.* [9] defined $Z_q(a)$ as the sum of the q -th powers of the local maxima of the modulus to avoid division by zero. We obtained the partition function $Z_q(a)$:

$$Z_q(a) = \sum |W_\varphi[f](a,b)|^q, \quad (1)$$

where $W_\varphi[f](a,b)$ is the wavelet coefficient of the function f , a is a scale parameter and b is a space parameter. The time window was set to six years for the following outlined reasons. We calculated the wavelets using a time window of various periods, 10, 6 and 4 years. For a time window of 10 years, a slow change of fractality was observed. Thus, this case was inappropriate to find a rapid change of climate indices because when we integrated the wavelet coefficient over a wide range, small changes were canceled. For four years, a fast change of

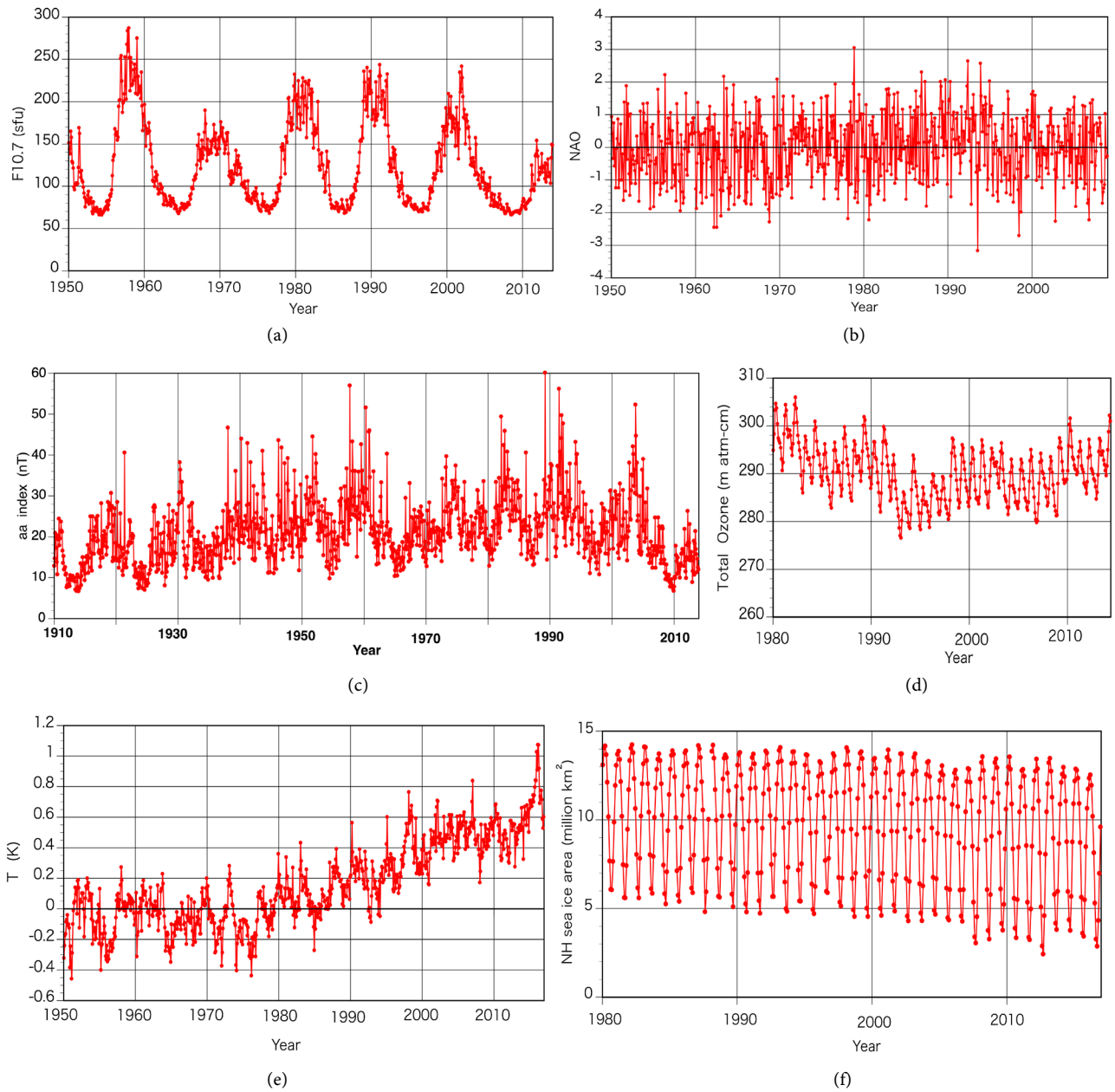


Figure 1. (a) The solar radio flux at 10.7 cm (F10.7 flux) provided by NOAA’s space weather prediction center; (b) The NAO index provided by NOAA’s Climate Prediction Center; (c) The geomagnetic aa index provided by NOAA; (d) The total ozone provided by NASA; (e) The global average temperature anomalies obtained from the Met Office Hadley Centre; (f) The NSIDC Sea Ice Index which shows the NH sea ice area.

fractality was observed. The overlap of the first and subsequent data was 3 years, which is shorter than the 9 years in the case of the 10-year calculation and thus the change of fractality was large. For six years, a moderate change of fractality was observed and hence the time window was set to this period. For small scales, we expect

$$Z_q(a) = a^{\tau(q)}. \tag{2}$$

First, we investigated the changes of $Z_q(a)$ in time series at a different scale a for each q . A plot of the logarithm of $Z_q(a)$ against the logarithm of time scale a was created. Here $\tau(q)$ is the slope of the linear fitted line on the log-log plot for each q . Next, we plotted $\tau(q)$ vs q . The time window was then shifted forward one year and the process repeated. We defined monofractal and multifractal as follows: if $\tau(q)$ is linear with respect to q , then the time series is said to be monofractal: if $\tau(q)$ is convex upwards with respect to q , then the time series is classified as multifractal [12]. We defined that the value of R^2 , which is the coefficient of determination, for fitting straight line, if $R^2 \geq 0.98$ the time series is monofractal and if $0.98 > R^2$ that is multifractal.

We calculated $\tau(q)$ for moments $q = -6, -5, -4, -3, -2, -1, 0, 1, 2, 3, 4, 5, 6$ for individual records for the SSN index. In **Figure 2**, $\tau(q)$ for individual SSN from 1967 to 1979 is shown. The data was analyzed in 6-year sets. For instance, $\tau(q)$ of s70 was calculated from 1970 to 1975, and that of s71 was calculated from 1971 to 1976. To detect the change of fractality, the time window was then shifted forward one year and $\tau(q)$ was calculated from s67 to s76. A monofractal signal corresponds to a straight line for $\tau(q)$, whereas for a multifractal signal, $\tau(q)$ is nonlinear. In **Figure 2**, $\tau(q)$ is linear for s69-s71, which indicates monofractality. In contrast, the nonlinear $\tau(q)$ curves for s67, s68, and s72-s74 show multifractality.

We plotted the value of the $\tau(-6)$ for each index. The negative large value of the $\tau(-6)$ shows large multifractality. For the $\tau(q)$, $q = -6$ is the appropriate number to show the change of τ . The value of the $\tau(-6)$ does not always correspond to the fractality obtained from the value of R^2 .

3. Results

3.1. The Influence of the Solar Activity on the NAO

To examine the influence of the solar activity on the NAO, we investigated the relation between the F10.7 flux and NAO index. The $\tau(-6)$ of the F10.7 flux, and NAO index are shown in **Figure 3** (top) and the SSN is also shown. The red square shows monofractality and the green circle shows multifractality for the 6 years centered on the year plotted. For instance, the green circle for 1980 in the SSN shows multifractality between 1977 and 1982. The data was excluded from **Figure 3** (top) for cases where we could not distinguish between monofractality and multifractality. When the SSN increased, the $\tau(-6)$ of the NAO was minimum and increased and the multifractality became weak. Especially, in 1998 when the 1998/1999 climatic regime shift occurred, the $\tau(-6)$ of the NAO was the smallest. When the SSN increased the $\tau(-6)$ of the F10.7 flux also increased and the solar activity became stable. Hence, when the SSN increased, the solar activity became stable and the NAO also became stable.

The lagged $\tau(-6)$ of the NAO was observed. This is consistent with the lagged North Atlantic climate response to solar variability [13]. The influence of the solar activity on the NAO was shown. For the 1990s, in the F10.7 flux and NAO

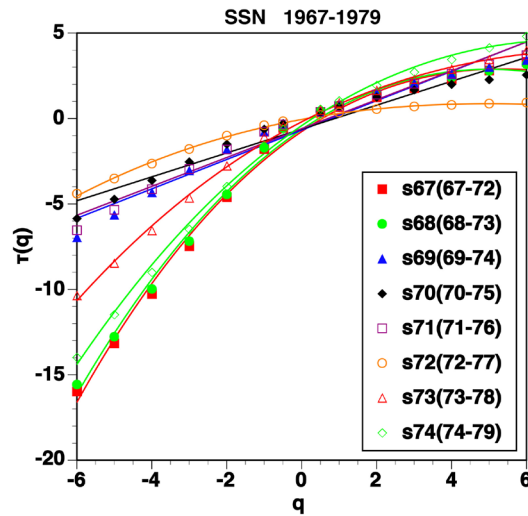


Figure 2. $\tau(q)$ for individual SSN between 1967 and 1979.

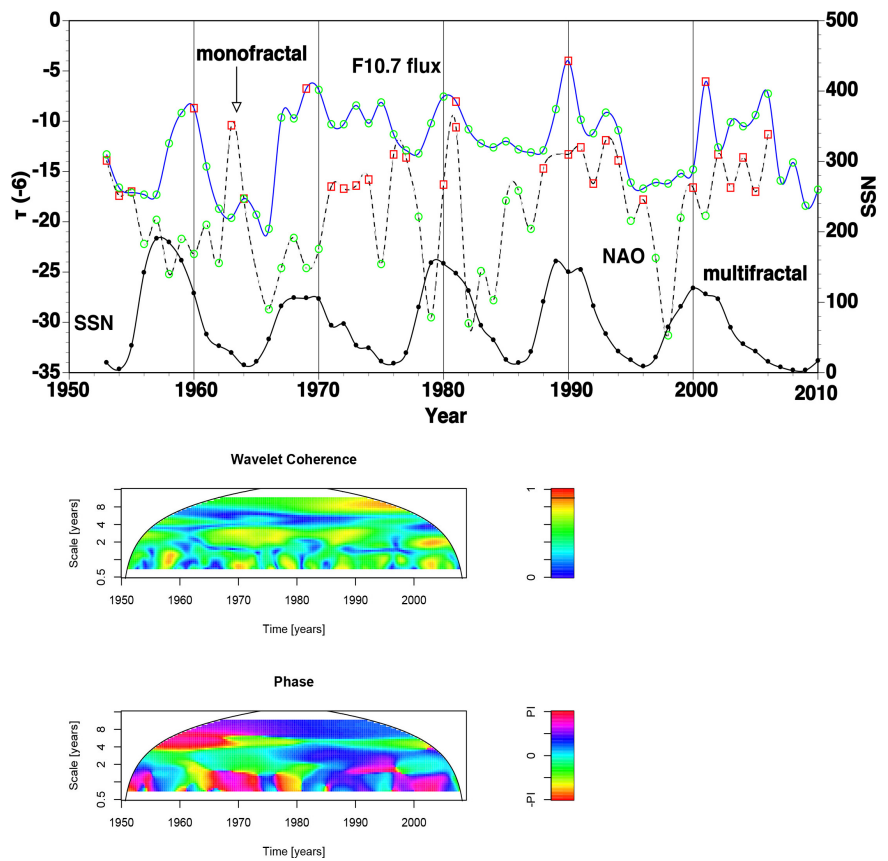


Figure 3. The $\tau(-6)$ of the F10.7 flux, and NAO index (top). The SSN is also shown. Wavelet coherence (middle) and phase (bottom) between the F10.7 flux and NAO index. The thick black contour encloses regions of greater than 95% confidence. The thin black contour encloses regions of greater than 90% confidence. The cone of influence, which indicates the region affected by edge effects, is shown with a black line. In the wavelet phase, the positive value shown by the blue and pink shading means that the F10.7 flux leads NAO index and the negative value shown by the green, yellow and red shading means that NAO index leads the F10.7 flux.

index, the matching in monofractality or multifractality was observed and the increase and decrease of multifractality were very similar, that is, the change of multifractality were very similar. When the SSN was maximum, the $\tau(-6)$ of F10.7 flux and NAO showed monofractal or weak multifractal. We investigated the relationship between the F10.7 flux and NAO index by means of wavelet coherence, and fractality. We show the wavelet coherence and phase using the Morlet wavelet between the F10.7 flux and NAO index in **Figure 3** (middle) and (bottom), respectively. The coherence between the F10.7 flux and NAO index in 8 year scale was strong since 1990, when both the changes of fractality were very similar and the lead of the F10.7 flux was observed. When the SSN was maximum, the coherence between F10.7 flux and NAO was strong in one year scale.

We obtained the $\tau(-6)$ of the SSN and NAO index and the wavelet coherence and phase using the Morlet wavelet between the SSN and NAO index. During the period 1950 and 2010, for the SSN and NAO index, the change of multifractality were very similar. The coherence between the SSN and NAO index in 8 year scale was strong since 1990, which showed the influence of solar activity. The lead of the SSN was observed.

For the SSN and F10.7 flux, the changes of multifractality were very similar. When the SSN became maximum, the fractality of the F10.7 flux changed from multifractality to monofractality for the solar cycles 20, 21, 22, and 23 in **Figure 3**.

3.2. The Influence of the Solar Flux on the Total Ozone

We investigated the relation between the F10.7 flux and total ozone. The $\tau(-6)$ of the F10.7 flux and total ozone are presented in **Figure 4** (top). During the period 1980 and 2010, for the F10.7 and total ozone, the change of multifractality were very similar. In monofractal the change is stable, and in multifractal the change is unstable. We show the wavelet coherence and phase using the Morlet wavelet between the F10.7 flux and total ozone in **Figure 4** (middle) and (bottom), respectively. The coherence between the F10.7 flux and total ozone in 4 - 8 year scale was strong for 1985-1995 as shown in **Figure 4** (middle) and the lead of the F10.7 flux was observed.

3.3. Relation between the NAO and Total Ozone

We investigated the relationship between the NAO index and total ozone. The $\tau(-6)$ of the NAO and total ozone are shown in **Figure 5** (top). During the period 1985 and 2010, for the NAO and total ozone, the change of multifractality were very similar. We show the wavelet coherence and phase using the Morlet wavelet between the NAO index and total ozone in **Figure 5** (middle) and (bottom), respectively. The coherence between the NAO and total ozone was strong and the leads of the total ozone and NAO index were observed.

3.4. Relation among the SSN, Geomagnetic Activity and NAO

We investigated the relation between the SSN and geomagnetic activity. The $\tau(-6)$ of the SSN and aa index, and the SSN are shown in **Figure 6** (top). The

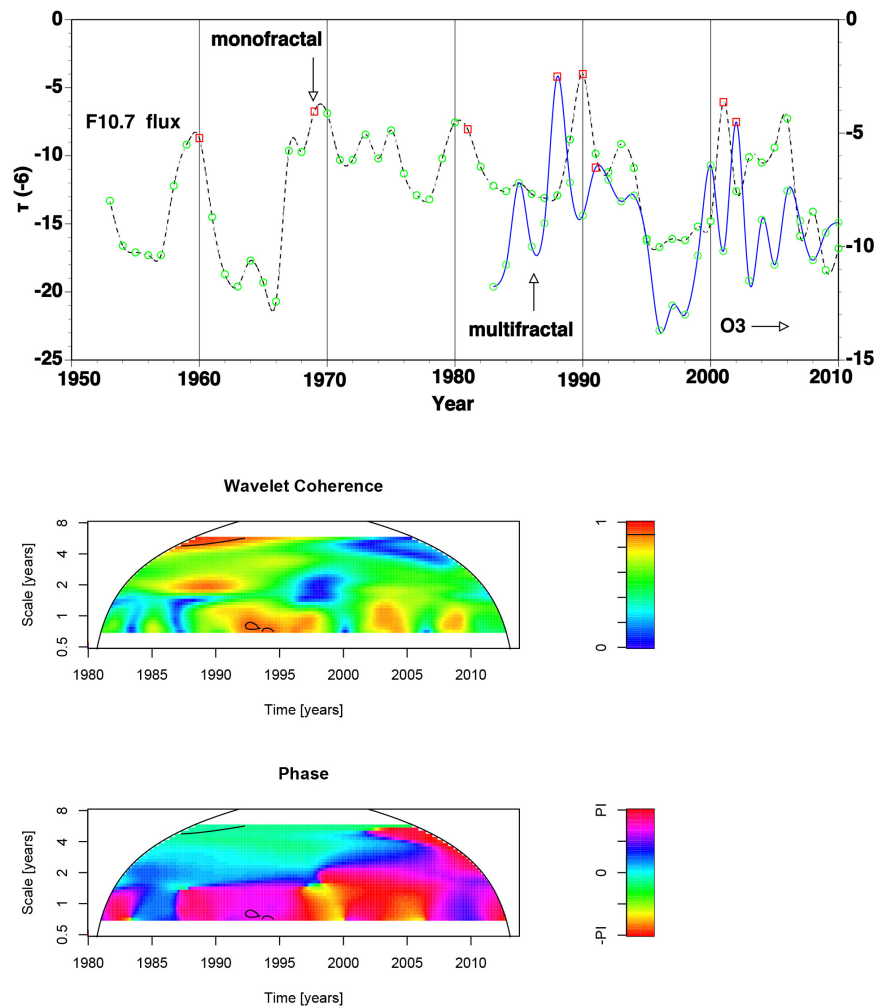


Figure 4. The $\tau(-6)$ of the F10.7 flux and total ozone (top). Wavelet coherence (middle) and phase (bottom) between the F10.7 flux and total ozone. In the wavelet phase, the positive value means that the F10.7 flux leads the total ozone and the negative value means that the total ozone leads the F10.7 flux.

$\tau(-6)$ of the SSN became minimum two years after the minimum SSN. During the period 1910 and 2010 except for 1960s, for the SSN and aa indices, the changes of multifractality were very similar for a long time. When the SSN increased, the $\tau(-6)$ of SSN and aa increased and showed weak multifractality. When the SSN was maximum, the $\tau(-6)$ of SSN and aa indices showed monofractality or weak multifractality. We show the wavelet coherence and phase using the Morlet wavelet between the SSN and aa index in **Figure 6** (middle) and (bottom), respectively. The coherence between the SSN and aa indices was strong in 11 year scale, which shows the influence of the solar activity on the geomagnetic activity, and the lead of the SSN was observed. Hence, the geomagnetic aa index can be used as the solar activity index.

We investigated the relationship between the NAO and geomagnetic activity, which shows the solar activity. The $\tau(-6)$ of the NAO and geomagnetic aa

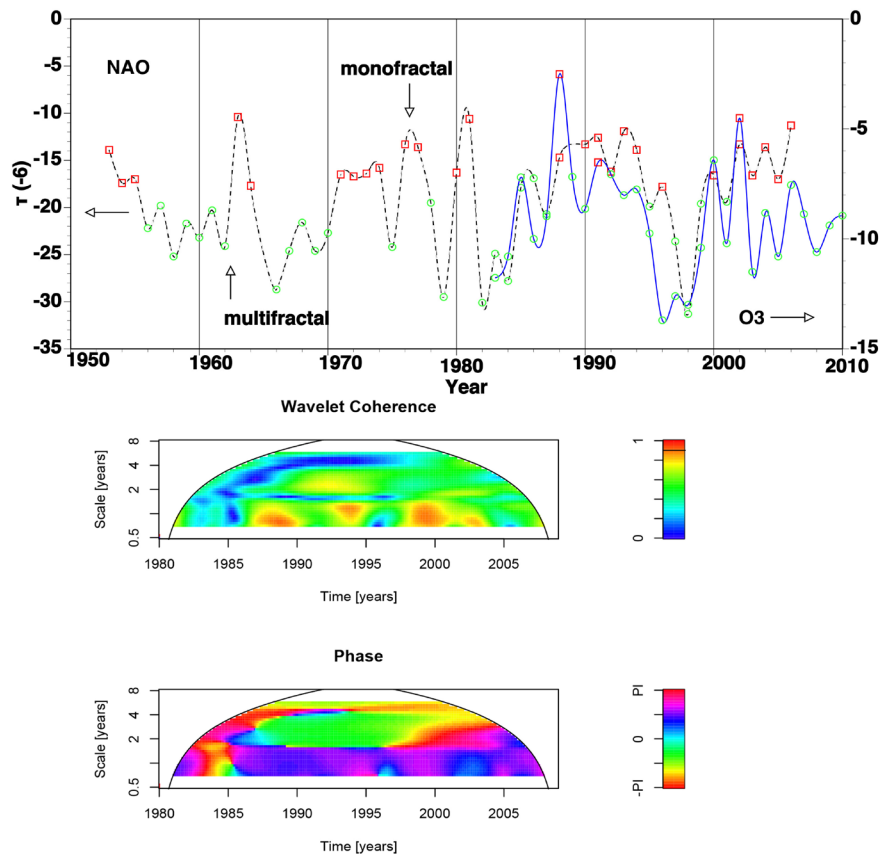


Figure 5. The $\tau(-6)$ of the NAO index and total ozone (top). Wavelet coherence (middle) and phase (bottom) between the NAO index and total ozone. In the wavelet phase, the positive value means that the NAO leads the total ozone and the negative value means that the total ozone leads the NAO.

indices are shown in **Figure 7**. During the period 1950 and 2010 except for 1990s, for the NAO and aa indices, the changes of multifractality were very similar and the lagged $\tau(-6)$ of the NAO was observed. This consists with the lagged North Atlantic climate response to solar variability [13]. We obtained the wavelet coherence and phase using the Morlet wavelet between the NAO and aa indices. The coherence between the NAO and aa indices was strong between 1980 and 2000 in 11 year scale, which showed the influence of the solar activity on the geomagnetic activity, and the lead of the aa index was observed since 1975.

3.5. Relation between the NAO and Global Temperature and between the NAO and NH Sea Ice Area

We investigated the relation between the NAO and the global temperature. The $\tau(-6)$ of the NAO and global temperature are presented in **Figure 8** (top). During the period 1950 and 2010, for the NAO and global temperature, the changes of multifractality were in excellent agreement. We show the wavelet coherence and phase using the Morlet wavelet between the NAO and global temperature in

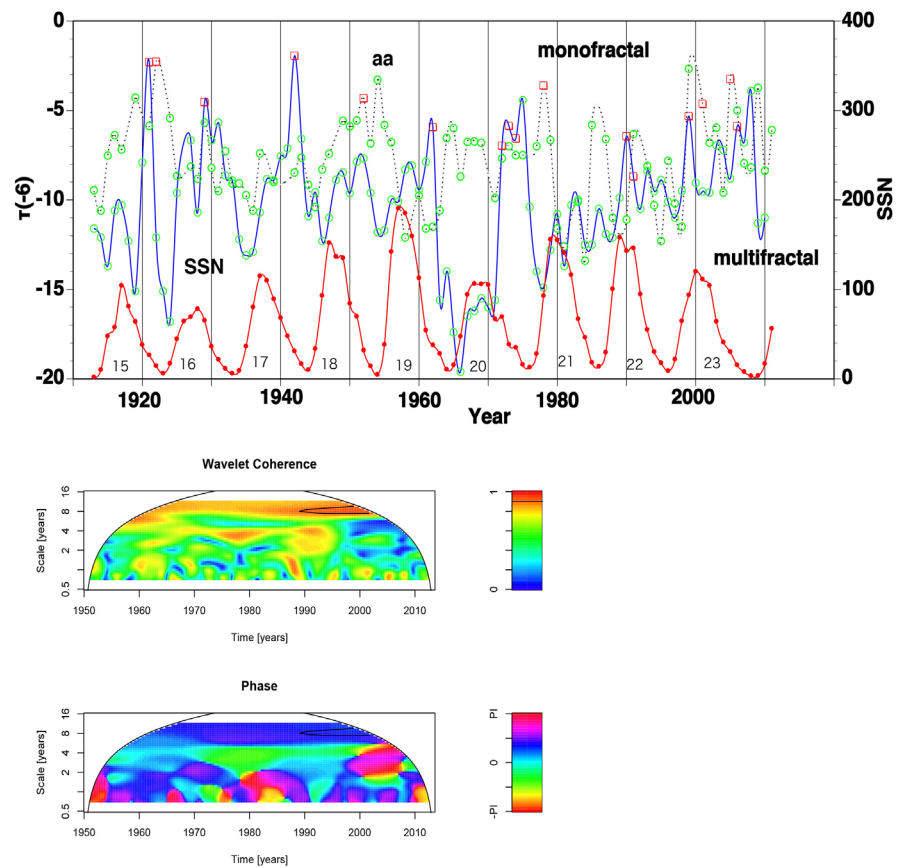


Figure 6. The $\tau(-6)$ of the SSN and aa index (top). The SSN and Solar cycle number of the SSN are also shown. Wavelet coherence (middle) and phase (bottom) between the SSN and aa index. In the wavelet phase, the positive value means that the SSN leads the aa index and the negative value means that the aa index leads the SSN.

Figure 8 (middle) and (bottom), respectively. The coherence between the NAO and global temperature was strong in one year scale, and the lead of the NAO was observed.

We examined the relation between the NAO and NH sea ice area. The $\tau(-6)$ of the NAO and NH sea ice area indices are shown in **Figure 9** (top). During the period 1980 and 2005, for the NAO and NH sea ice area indices, the changes of multifractality were very similar. We show the wavelet coherence and phase using the Morlet wavelet between the NAO and NH sea ice area indices in **Figure 9** (middle) and (bottom), respectively. The coherence between the NAO and NH sea ice area indices was strong in one year scale, and the lead of the NAO was observed.

4. Discussion

4.1. The Relation among the Solar Activity, Total Ozone, and NAO

Fractal behavior may be observed in many self-organization systems, representing the order or disorder included in the systems. There is a model that

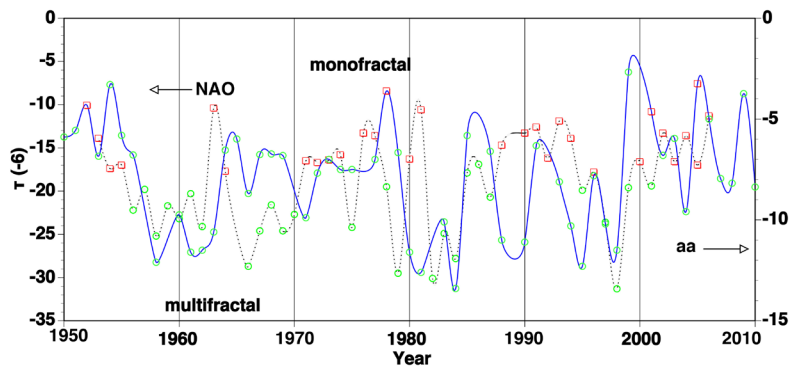


Figure 7. The $\tau(-6)$ of the NAO and aa indices.

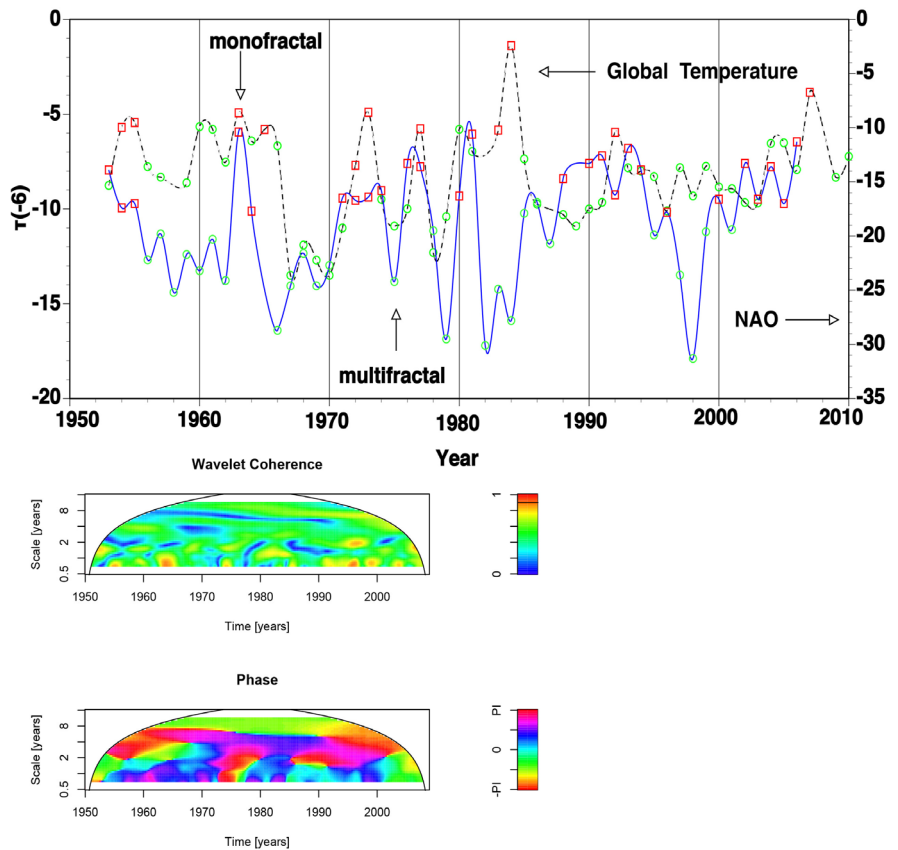


Figure 8. The $\tau(-6)$ of the NAO and global temperature (top). Wavelet coherence (middle) and phase (bottom) between the NAO and global temperature. In the wavelet phase, the positive value means that the NAO leads the global temperature and the negative value means that the global temperature leads the NAO.

deals with an interaction between magnetism and fluid [14]. It is reported that a phenomenon of self-organization occurs and a fractal is observed. Their model was performed in a micro level, but a similar mechanism might occur in an interaction between the Earth and Sun. Therefore, the study of fractals becomes an important issue to assess a relation between the solar activity and the Earth's climate.

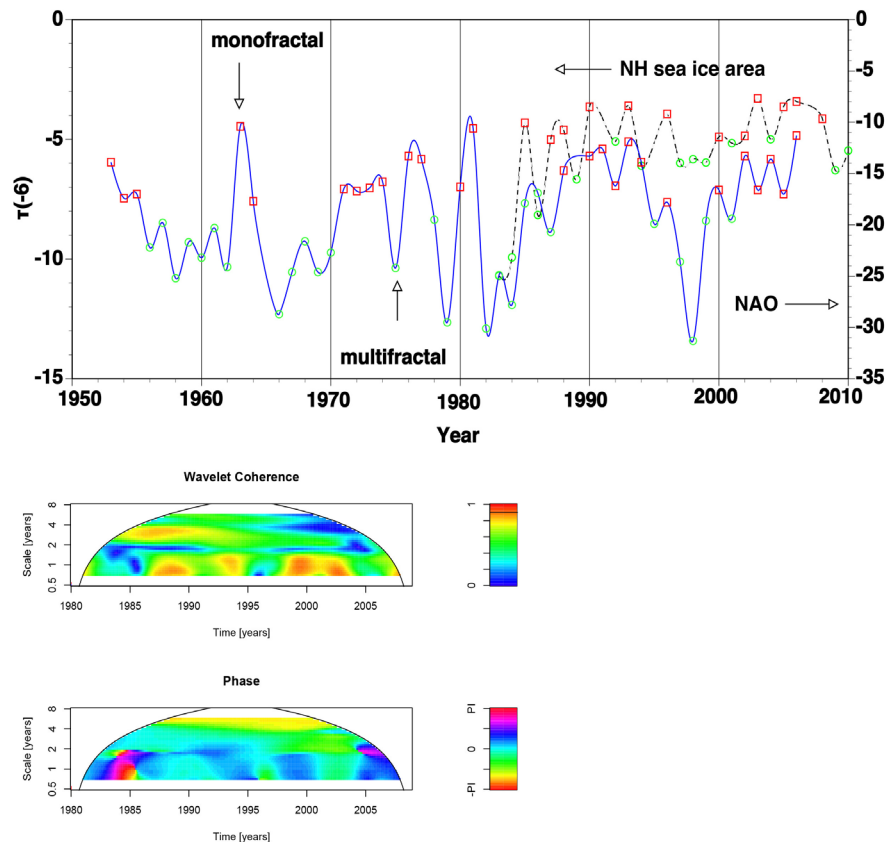


Figure 9. The $\tau(-6)$ of the NAO and NH sea ice area indices (top). Wavelet coherence (middle) and phase (bottom) between the NAO and NH sea ice area indices. In the wavelet phase, the positive value means that the NAO leads the NH sea ice area index and the negative value means that the NH sea ice area index leads the NAO.

When the SSN increased, the solar activity became stable and the NAO also became stable. The relation between the solar activity and the NAO was shown. When the SSN became maximum, the fractality of the F10.7 flux changed from multifractality to monofractality for the solar cycles 20, 21, 22, and 23 in **Figure 3**.

During the period 1980 and 2010, for the F10.7 and total ozone, the matching in monofractality or multifractality was observed and the increase and decrease of multifractality were very similar, that is the changes of multifractality were very similar.

When the SSN became maximum, the fractality of the total ozone changed from multifractality to monofractality. The coherence between the F10.7 flux and total ozone in 4 - 8 year scale was strong for 1985-1995 and the lead of the F10.7 flux was observed. The influence of the solar activity on the total ozone was shown by the wavelet coherence, and the similarity of the change of fractality.

During the period 1985 and 2010, for the NAO and total ozone, the changes of multifractality were very similar. When the SSN became maximum, the fractality

of the NAO changed from multifractality to monofractality for the solar cycles 21, 22, and 23 in **Figure 3**. The coherence between the NAO index and total ozone was strong and the leads of the total ozone and NAO index were observed. Those consisted with the results that the influence of total ozone to atmospheric field is shown [15] and the NAO is modulating the Earth's ozone shield [16].

When the SSN was maximum, the $\tau(-6)$ of F10.7 flux and NAO showed monofractal or weak multifractal and the coherence between F10.7 flux and NAO was strong in one year scale. Those consisted with the result of Kodera [17] as below. The spatial structure of the NAO differs significantly according to the phase of the solar cycle. During the solar maximum phases, the NAO has a hemispherical structure extending into the stratosphere.

The lagged North Atlantic climate response to solar variability is shown [13]. After a solar maximum, the positive phase of the NAO is observed [18]. This suggests the presence of inter annual memory, perhaps residing in the Atlantic Ocean.

We show the absolute value of $\tau(-6)$ for F10.7 flux, total ozone, and NAO in **Figure 10**. The vertical axis is natural logarithmically transformed. The change rate for all indices was similar. Especially, the changes of all indices were very similar for 1990s and the relation among them was shown. The negative large value of the $\tau(-6)$ shows large multifractality and instability. When the solar activity was strong, the absolute value of $\tau(-6)$ for F10.7 flux was small and solar activity was stable, and the absolute value of $\tau(-6)$ of total ozone was small. Hence the changes of F10.7 flux and total ozone were related. The $\tau(-6)$ for F10.7 flux and NAO was related each other, and the lagged $\tau(-6)$ of the NAO was observed. It was found that the multifractality was strong in the order of NAO, F10.7 flux and total ozone, and it was found to have an unstable change.

The relation among the solar activity, the total ozone, and the NAO were shown by the wavelet coherence, and the similarity of the change of fractality. The influence of the solar activity on the NAO was shown.

4.2. The Influence of the Solar Activity on the NAO

For the NAO and aa indices, the changes of multifractality were very similar between 1950 and 2010. When the SSN became maximum, the fractality of the aa index changed from multifractality to monofractality for the solar cycles 20, 21, 22, and 23 in **Figure 7**. The coherence between the NAO and aa indices was strong and the lead of the aa index was observed. The influence of the aa index on the NAO was shown by the wavelet coherence, and the similarity of the change of fractality. The correlation between the geomagnetic Ap and NAO indices is high and significant since about 1970 [7].

For the aa index and SSN, the change of multifractality were very similar between 1910 and 2010. When the SSN became maximum, the fractality of the SSN changed from multifractality to monofractality. The coherence between the aa

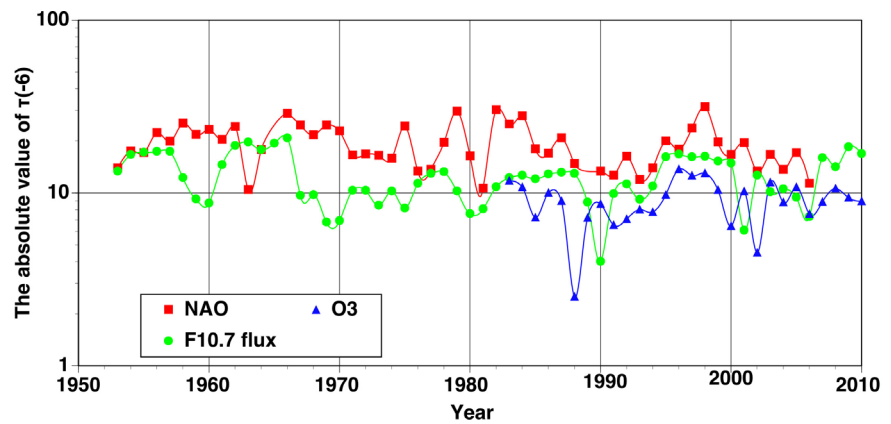


Figure 10. The absolute value of $\tau(-6)$ for F10.7 flux, total ozone, and NAO indices. The vertical axis is natural logarithmically transformed.

index and SSN was strong in 11 year scale and the lead of the SSN was observed. The influence of the SSN on the aa index was shown by the wavelet coherence, and the similarity of the change of fractality.

Disturbances in the geomagnetic field were small when solar activity was not active.

When the SSN was maximum or minimum, the $\tau(-6)$ of the aa index became maximum and the geomagnetic field showed weak multifractality. Two years before the maximum SSN, the $\tau(-6)$ of the aa index became minimum. These results show a similar tendency of $\tau(-6)$ for the SSN and solar polar field strength, which indicates that solar activity influences geomagnetic activity. The greater the geomagnetic disturbance, the larger the maximum SSN of the next cycle [11]. The relation between the solar activity and the geomagnetic activity was shown clearly by the wavelet coherence and phase and the similarity of the change of fractality. When the SSN became maximum, the fractality of the SSN, F10.7 flux, geomagnetic aa, and NAO indices changed from multifractality to monofractality and those states became stable.

In a coupled chaos model, where a coupled chaos is a system composed of chaos which interact with each other, an anomalous enhancement of the magnitude of a fluctuation is observed at the phase synchronization point [19]. In other words, an increase of a fluctuation is observed in a coupled chaos system just before chaos synchronization, which is when fractality and state change. Coupled chaotic systems have attracted the attention of many researchers as a good model which can realize the complicated phenomena of the natural world, and further its dynamics can yield a wide variety of complex and strange phenomena [20]. For the SSN maximum, a mechanism similar to the coupled chaos system might exist, *i.e.*, coherence becomes strong and fluctuations increase, and the multifractal behavior becomes strong and a change from multifractal to monofractal behavior is observed. This implies that strong interactions of the solar flux, geomagnetic activity, total ozone, and NAO occur in the SSN maxi-

mum. The strong interactions were inferred from the similarity of fractality changes and the wavelet coherence. The influence of the solar activity on the NAO was shown.

4.3. Relation between the NAO and Global Temperature, and between the NAO and NH Sea Ice Area

We investigated the relation between the NAO and the global temperature. Recent studies have suggested that sea surface temperature (SST) is an important source of variability of the NAO [21]. For the NAO and global temperature, the changes of multifractality were very similar between 1950 and 2010. The coherence between the NAO and global temperature was strong in one year scale, and the lead of the NAO was observed.

It has been suggested that the atmospheric circulation might be affected by sea ice [22]. Sea ice is a critical component of the climate system because it strongly influences albedo, surface turbulent heat fluxes, surface wind drag, and upper-ocean stratification. We investigated the relation between the NAO and NH sea ice area. For the NAO and NH sea ice area, the changes of multifractality were very similar between 1980 and 2005. The coherence between the NAO and NH sea ice area indices was strong in one year scale, and the lead of the NAO was observed. Sea ice is a sensitive component of the climate system, influenced by conditions in both the atmosphere and ocean [23]. The winter sea ice is about 50 cm thinner in high NAO index years than in lower NAO index years in the Eurasian coastal region mainly due to stronger wind-driven ice export [24].

The relation between the NAO and global temperature, and between the NAO and NH sea ice area were shown clearly by the wavelet coherence, and the similarity of the change of fractality. The wavelet coherence between the NAO and NH sea ice area indices was stronger than that between the NAO and global temperature. Sea ice variations induce a greater atmospheric response associated with the NAO than variations in SST does [25].

5. Conclusions

We examined the relationship among the solar activity, total ozone, and the NAO from a viewpoint of multi-fractality. We investigated the change of multi-fractal behavior of the SSN, F10.7 flux, geomagnetic aa, total ozone, NAO, the global temperature, and NH sea ice area indices by the multifractal analysis using the wavelet transform. For this purpose, we illustrated the change of multifractality by plotting the τ -function and used the wavelet coherence. The main findings are summarized below.

- 1) When the SSN increased, the solar activity became stable and the NAO also became stable. The lagged fractality of NAO was observed. During the period 1950 and 2010, for the SSN and NAO, the matching in monofractality or multifractality was observed and the increase and decrease of multifractality of these indices coincided with each other. When the SSN became maximum, the fractal-

ity of the SSN, F10.7 flux, geomagnetic aa, and NAO indices changed from multifractality to monofractality and those states became stable for most of the solar cycles. The relationship among the solar activity, the total ozone, and the NAO were shown by the similarity of fractality changes and the wavelet coherence.

2) An increase of a fluctuation is observed in a coupled chaotic system just before chaos synchronization, which is when fractality and state change. We expect that a similar mechanism might exist for the SSN maximum. When the SSN became maximum, the fluctuations became large and multifractality became strong, and a change from multifractal to monofractal behavior was observed in the SSN, F10.7 flux, geomagnetic aa, and NAO indices. The strong interactions of the solar flux, geomagnetic activity, total ozone, and NAO occur in the SSN maximum. The strong interactions were inferred from the similarity of fractality changes and the wavelet coherence. The influence of the solar activity on the NAO was shown from a viewpoint of multi-fractality.

3) The similar coincidences of multifractal behavior were also shown between the SSN and geomagnetic aa index, between the NAO and global temperature, and between the NAO and NH sea ice area.

These findings will contribute to the research of the relation between the solar activity and climate change.

Conflicts of Interest

The authors declare no conflicts of interest regarding the publication of this paper.

References

- [1] Lean, J.L., Rottman, G.L., Kyle, H.L., Woods, T.N., Hickey, J.R. and Puga, L.C. (1997) Detection and Parameterization of Variations in Solar Mid and Near Ultraviolet Radiation (200 to 400 nm). *Journal of Geophysical Research*, **102**, 29939-29956. <https://doi.org/10.1029/97JD02092>
- [2] Kodera, K. and Kuroda, Y. (2002) Dynamical Response to the Solar Cycle. *Journal of Geophysical Research*, **107**, 4749. <https://doi.org/10.1029/2002JD002224>
- [3] Neff, U., Burns, S.J., Mangini, A., Mudelsee, M., Fleitmann, D. and Matter, A. (2001) Strong Coherence between Solar Variability and the Monsoon in Oman between 9 and 6 Kyr Ago. *Nature*, **411**, 290-293. <https://doi.org/10.1038/35077048>
- [4] Hood, L.L., Soukharev, B.E. and McCormack, J.P. (2010) Decadal Variability of the Tropical Stratosphere: Secondary Influence of the El Niño-Southern Oscillation. *Journal of Geophysical Research*, **115**, D11113. <https://doi.org/10.1029/2009JD012291>
- [5] Boberg, F. and Lundstedt, H. (2003) Solar Wind Electric Field Modulation of the NAO: A Correlation Analysis in the Lower Atmosphere. *Geophysical Research Letters*, **30**. <https://doi.org/10.1029/2003GL017360>
- [6] Fujita, R. and Tanaka, H.L. (2007) Statistical Analysis on the Relationship between Solar and Geomagnetic Activities and the Arctic Oscillation. *Journal of the Meteorological Society of Japan*, **85**, 909-918.
- [7] Thejll, P., Christiansen, B. and Gleisner, H. (2002) On Correlation between the North Atlantic Oscillation, Geopotential Heights, and Geomagnetic Activity. *Geo-*

- physical Research Letters*, **30**. <https://doi.org/10.1029/2002GL016598>
- [8] Svensson, C., Olsson, J. and Berndtsson, R. (1996) Multifractal Properties of Daily Rainfall in Two Different Climates. *Water Resources Research*, **32**, 2463-2472. <https://doi.org/10.1029/96WR01099>
- [9] Muzy, J.F., Bacry, E. and Arneodo, A. (1991) Wavelets and Multifractal Formalism for Singular Signals: Application to Turbulence Data. *Physical Review Letters*, **67**, 3515-3518. <https://doi.org/10.1103/PhysRevLett.67.3515>
- [10] Maruyama, F., Kai, K. and Morimoto, H. (2015) Wavelet-Based Multifractal Analysis on Climatic Regime Shifts. *Journal of the Meteorological Society of Japan*, **93**, 331-341.
- [11] Maruyama, F., Kai, K. and Morimoto, H. (2017) Wavelet-Based Multifractal Analysis on a Time Series of Solar Activity and PDO Climate Index. *Advances in Space Research*, **60**, 1363-1372. <https://doi.org/10.1016/j.asr.2017.06.004>
- [12] Frish, U. and Parisi, G. (1985) On the Singularity Structure of Fully Developed Turbulence, in *Turbulence and Predictability in Geophysical Fluid Dynamics and Climate Dynamics*. In: Ghil, M., Benzi, R. and Parisi, G., Eds., North-Holland, New York, 84-88.
- [13] Scaife, A.A., Ineson, S., Knight, J.R., Gray, L., Kodera, K. and Smith, D.M. (2013) A Mechanism for Lagged North Atlantic Climate Response to Solar Variability. *Geophysical Research Letters*, **40**, 434-439. <https://doi.org/10.1002/grl.50099>
- [14] Bartosz, A.G., Howard, A.S. and George, M.W. (2000) Dynamic Self-Assembly of Magnetized, Millimetre-Sized Objects Rotating at a Liquid-Air Interface. *Nature*, **405**, 1033-1036. <https://doi.org/10.1038/35016528>
- [15] Thompson, D.W.J. and Solomon, S. (2002) Interpretation of Recent Southern Hemisphere Climate Change. *Science*, **296**, 895-899. <https://doi.org/10.1126/science.1069270>
- [16] Appenzeller, C., Weiss, A.K. and Staehelin, J. (2000) North Atlantic Oscillation Modulates Total Ozone Winter Trends. *Geophysical Research Letters*, **27**, 1131-1134. <https://doi.org/10.1029/1999GL010854>
- [17] Kodera, K. (2002) Solar Cycle Modulation of the North Atlantic Oscillation: Implication in the Spatial Structure of the NAO. *Geophysical Research Letters*, **29**, 1218. <https://doi.org/10.1029/2001GL014557>
- [18] Gray, L.J., Scaife, A.A., Mitchell, D.M., Osprey, S., Ineson, S., Hardiman, S., Butchart, N., Knight, J., Sutton, R. and Kodera, K. (2013) A Lagged Response to the 11 Year Solar Cycle in Observed Winter Atlantic/European Weather Patterns. *Journal of Geophysical Research: Atmospheres*, **118**, 13405-13420. <https://doi.org/10.1002/2013JD020062>
- [19] Fujisaka, H., Uchiyama, S. and Horita, T. (2005) Mapping Model of Chaotic Phase Synchronization. *Progress of Theoretical Physics*, **114**, 289-299. <https://doi.org/10.1143/PTP.114.289>
- [20] Wada, M., Kitatsuji, K. and Nishio, Y. (2005) Spatio-Temporal Phase Patterns in Coupled Chaotic Maps with Parameter Deviations. *Proceedings of 2005 International Symposium on Nonlinear Theory and Its Applications*, Bruges, 18-21 October 2005, 178-181.
- [21] Paeth, H., Latif, M. and Hense, A. (2003) Global SST Influence on Twentieth Century NAO Variability. *Climate Dynamics*, **21**, 63-75. <https://doi.org/10.1007/s00382-003-0318-4>

- [22] Alexander, M.A., Bhatt, U.S., Walsh, J.E., Timlin, M.S., Miller, J.S. and Scott, J.D. (2004) The Atmospheric Response to Realistic Arctic Sea Ice Anomalies in an AGCM during Winter. *Journal of Climate*, **17**, 890-905.
[https://doi.org/10.1175/1520-0442\(2004\)017<0890:TARTRA>2.0.CO;2](https://doi.org/10.1175/1520-0442(2004)017<0890:TARTRA>2.0.CO;2)
- [23] Deser, C., Walsh, J.E. and Timlin, M.S. (2000) Arctic Sea Ice Variability in the Context of Recent Atmospheric Circulation Trends. *Journal of Climate*, **13**, 617-633.
[https://doi.org/10.1175/1520-0442\(2000\)013<0617:ASIVIT>2.0.CO;2](https://doi.org/10.1175/1520-0442(2000)013<0617:ASIVIT>2.0.CO;2)
- [24] Hu, A., Rooth, C., Bleck, R. and Deser, C. (2002) NAO Influence on Sea Ice Extent in the Eurasian Coastal Region. *Geophysical Research Letters*, **29**, 10-1-10-4.
<https://doi.org/10.1029/2001GL014293>
- [25] Magnusdottir, G., Deser, C. and Saravanan, R. (2004) The Effects of North Atlantic SST and Sea Ice Anomalies on the Winter Circulation in CCM3. Part 1: Main Features and Storm Track Characteristics of the Response. *Journal of Climate*, **17**, 857-876.
[https://doi.org/10.1175/1520-0442\(2004\)017<0857:TEONAS>2.0.CO;2](https://doi.org/10.1175/1520-0442(2004)017<0857:TEONAS>2.0.CO;2)